Available online at www.sciencedirect.com
ScienceDirect
Composite Structures 84 (2008) 29–43
COMPOSITE STRUCTURES
www.elsevier.com/locate/compstruct

# Composite behavior of hybrid FRP-concrete bridge decks on steel girders

Wael Alnahhal [a], Amjad Aref [b,*], Sreenivas Alampalli [c]

[a] Halcrow Yolles, 207 Queen's Quay West, Suite 550, PO Box 132, Toronto, ON, Canada M5J 1A7
[b] Department of Civil, Structural and Environmental Engineering, University at Buffalo, 235 Ketter Hall, Buffalo, NY 14260, United States
[c] Bridge Evaluation Services Bureau, New York State, Department of Transportation, Albany, NY 12232, United States

Available online 5 July 2007

**Abstract**

A hybrid FRP-concrete deck on steel girders specimen was subjected to a series of service flexural loading tests under seven different loading conditions to capture the global response of the specimen, and to investigate the composite action of the bridge. The experimental and finite element results demonstrated that the structural performance of the hybrid FRP-concrete bridge deck exceeds AASHTO specifications. In addition, it was observed that the hybrid deck and the steel girders are interacting in a partially composite action under service loading conditions. Effective width calculations of the hybrid deck showed that the effective flange width for hybrid decks are less than AASHTO prescribed effective width for concrete decks.


*Keywords:* FRP composites; Concrete; Bridge deck; Composite structures; Effective flange width; Finite element analysis

## 1. Introduction

The United States (US) has one of the largest highway networks in the world. The efficiency and safety of this network plays an essential role in the continued economic vitality of the country. The total number of bridges in the US as of 2003 is 615,718 [10], and nearly 26.3% of these bridges are either structurally deficient or functionally obsolete. There is, however, a major challenge to reduce or eliminate deficient structures. A solution to this challenge may be to use new materials or to implement new structural systems. Among new structural materials, FRP composites have continued to play an important role in solving some of the persistent problems in infrastructure applications due to their superior material properties such as high specific stiffness, high specific strength, high corrosion resistance, light weight, and durability.

Based on these advantages and a wide variety of practical applications, the composites industry has grown approximately 460% over the past 30 years, from 360,000 tons in 1970 to 1.68 million tons in 2000 [8]. In spite of all these advantages, FRP composites have higher initial costs than conventional materials used in infrastructure applications. To overcome this obstacle and to make the best use of materials, combinations of FRP and conventional materials have recently been investigated by a number of researchers [3]. The advantages of hybrid structural systems include the cost effectiveness and the ability to optimize the cross-section based on material properties of each constituent material.

According to Mirmiran [21], the most effective use of FRP composites is in the form of hybrid construction with concrete, where FRP acts as a load carrying constituent and a protective measure for concrete. Seible et al. [27] investigated a two span bridge with light weight concrete filled circular CFRP composite tubes. Their preliminary estimates indicate that two different bridge systems (the concrete filled CFRP beams with reinforced concrete

* Corresponding author. Tel.: +1 716 645 2114x2423.
*E-mail addresses:* aaref@eng.buffalo.edu (A. Aref), salampalli@dot.state.ny.us (S. Alampalli).

0263-8223/$ - see front matter © 2007 Elsevier Ltd. All rights reserved.
doi:10.1016/j.compstruct.2007.06.005

(RC) deck and the concrete filled CFRP beams with pultruded modular E-glass deck) are 20% and 100% more expensive, respectively, when compared to a conventional RC slab bridge.

The hybrid deck system proposed in this study consists of trapezoidal cell units surrounded by an outer shell forming an integral bridge deck. A thin layer of concrete was placed in the compression zone of the section. Concrete was confined by glass fiber reinforced polymer (GFRP) laminates that protect it from the environmental exposure and hence delays or prevents the onset of damage. One of the most likely uses of the proposed hybrid FRP-concrete bridge system is for bridge decks over steel or concrete girders. In this application, the hybrid deck replaces traditional steel reinforced concrete decks. To be efficiently used in modern bridge decking application, the proposed hybrid deck must be made to act compositely with steel girders. Thus, a sufficiently robust shear transfer interface at the hybrid deck to steel transition zone is required. In this study, welded shear studs were used to connect the hybrid deck to steel girders.

In this paper, we present a detailed description of a 3/4 scale steel bridge model with hybrid FRP-concrete deck followed by the results of a series of service-level flexural loading tests. The experimental results are then used to validate the finite element analysis (FEA). The composite action between the hybrid deck and steel girders is investigated analytically and validated by test data. Moreover, the effective flange width in the hybrid FRP-concrete deck acting compositely with the steel girders is evaluated at service conditions.

## 2. Hybrid FRP-concrete bridge deck

The proposed hybrid FRP-concrete bridge deck consists of trapezoidal cell units surrounded by an outer shell (see Fig. 1). According to Ashby [6], thin walled box sections represent the most efficient structural forms for beams. A thin layer of concrete was placed in the compression zone of the section. Concrete was confined by GFRP laminates that provide protection from environmental exposure. In addition to enhancing the stiffness of the deck, the concrete layer reduces the local deformation of the top surface of the bridge under concentrated loads that represent truck wheel loads. Trapezoidal box sections with an inclination angle impart reduced shear stresses at the interface of adjacent box sections. According to Kitane and Aref [17], the inclination of 3/8 has the smallest deformation at the riding surface. Thus, inclination of 3/8 was chosen for the proposed bridge deck system. To evaluate the efficacy of the proposed bridge deck system, a prototype bridge system (6.5 m long and 4.06 m wide) was designed as a simply supported steel bridge with a hybrid FRP-concrete deck. The height of the hybrid deck was limited to 200 mm so that the proposed deck can be used for deck renewal projects. This proposed bridge system has several inherent advantages over an all FRP composite bridge, which can be summarized in the following points:

- GFRP is corrosion-resistant whereby concrete is protected from any potential harsh environmental exposure; thus, the system will require less maintenance than conventional bridges.
- Concrete is designed to be always in compression in the longitudinal direction. The fact that concrete is not used in the tension side leads to significant weight reduction when compared to a concrete-filled FRP section.
- It has been reported that the local deformation under concentrated point loads resulting form truck wheels may become large for all-composite bridge decks [5,7]. A layer of concrete can effectively reduce this local deformation of the top flange and improve the serviceability of the wearing surface.

## 3. Test specimen

The test specimen was a 3/4 scale model of the 6.5 m prototype steel bridge. The model had a length of 4.88 m.

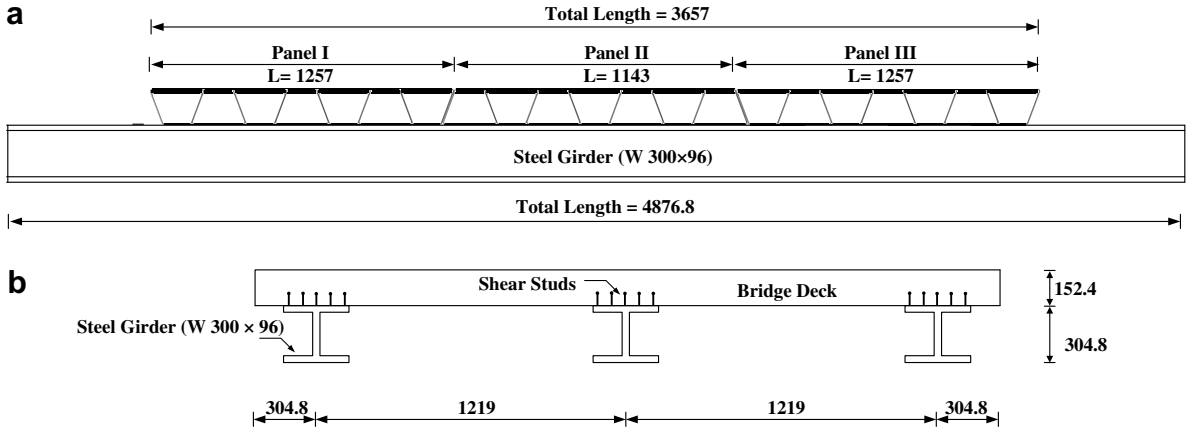


Fig. 1. 3/4 scale model of steel bridge with a hybrid FRP-concrete bridge deck (units in mm) (a) elevation and (b) side view.

The deck model supported on steel girders had a length of 3.05 m, a width of 3.66 m, and a depth of 150 mm. The hybrid FRP-concrete deck specimen (FRP part only) was fabricated at An-Cor Industrial Plastics, Inc., N. Tonawanda, NY. Both elevation and side views of the steel bridge with the hybrid FRP-concrete deck are illustrated in Fig. 1.

The hybrid bridge deck was comprised of three deck panels, and each panel had seven trapezoidal cross-sections surrounded by an outer shell. A thin layer of concrete was placed in the compression zone of each section. Each trapezoidal section consisted of two layers of laminates (glass fibers and vinyl ester matrix): the inner tube laminate and the outer tube laminate. The inner tube with glass fiber orientations of $[0°_4]$, was first constructed, and the outer tube was then laminated over the inner tube laminate with a laminate construction $[0°_3]$. The outermost laminate stacking sequence was $[0°_5]$. Table 1 shows the stacking sequence and thickness of various components of the bridge deck model. As mentioned above, the stacking sequence chosen for all laminates was 0°. This selection was made because the woven fabric type chosen as reinforcement in this study has almost the same mechanical properties in the two orthogonal directions.

Each trapezoidal box section was fabricated individually by the hand lay-up process. Consequently, the seven trapezoidal sections were then assembled by using the vacuum bag process. A layer of glass fiber chopped strand mat wetted with vinyl ester resin was applied between box sections to enhance the bonding at the interface between the sections, and to allow for a better bond if there exists mismatch between the surfaces being bonded. The seven trapezoidal sections were then wrapped with the outermost laminate to form the integral deck unit.

To achieve good composite action between GFRP laminates and concrete, shear keys, were installed in staggered positions at the interface of the GFRP laminates and concrete. Each shear key had a length of 0.155 m for the side trapezoidal section and 0.076 m for the middle trapezoidal section in the transverse direction to effectively transfer the shear stress across the concrete-FRP interface. The shear keys were installed on the top surface of the inner tube laminate and on the bottom surface of the outer tube laminate with an interval of 0.508 m. These shear keys were also made of GFRP composites.

The final stage of constructing the deck panels entails the placement of the concrete layer in the cavity that was created during the lamination process. The concrete was poured at the civil engineering laboratory at University at Buffalo. Foam dams were firstly placed in the shear studs holes (see Fig. 2) to avoid leaking of concrete. The cavities were filled completely with concrete. Mechanical properties

Table 1
Thickness and stacking sequence of the hybrid deck model

| | Stacking sequence | Thickness (mm) |
|---|---|---|
| Inner tube laminate | $[0°_4]$ | 1.524 |
| Outer tube laminate | $[0°_3]$ | 1.143 |
| Outer-most tube laminate | $[0°_5]$ | 1.905 |

Table 2
Tensile properties of GFRP

| Direction | Coupon | Modulus of elasticity (GPa) | Tensile strength (MPa) | Ultimate strain |
|---|---|---|---|---|
| Fill | Fill-1 | 16.38 | 339.64 | 0.0267 |
| | Fill-2 | 16.02 | 339.64 | 0.0267 |
| | Fill-3 | 16.21 | 339.50 | 0.0267 |
| | Average | 16.20 | 339.57 | 0.0267 |
| Warp | Warp-1 | 15.48 | 299.72 | 0.0262 |
| | Warp-2 | 16.19 | 285.44 | 0.0232 |
| | Warp-3 | 15.96 | 293.30 | 0.0255 |
| | Average | 15.88 | 292.82 | 0.0250 |

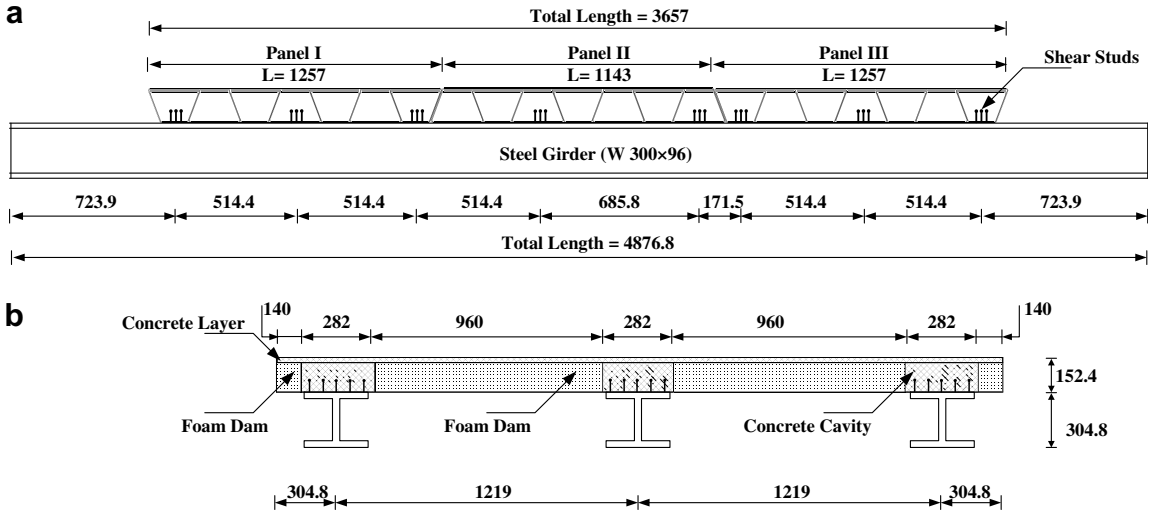


Fig. 2. Shear stud configuration (units in mm) (a) elevation and (b) cross-section.

Table 3
Mechanical properties of concrete

| Specimen | Strength, $f'_c$ (MPa) | Chord modulus of elasticity (GPa) |
|---|---|---|
| Sp-1 | 57.10 | 31.43 |
| Sp-2 | 57.20 | 31.90 |
| Sp-3 | 52.60 | 28.30 |
| Average | 55.63 | 30.50 |

of both GFRP composites and concrete used in this study [2] are listed in Tables 2 and 3, respectively.

As seen in Fig. 1, the hybrid FRP decks were connected to a typical steel bridge. The bridge consisted of three W-beam girders (W300 × 96). The girders were spaced at 1.22 m center-to-center, and the deck overhang was 0.305 m for the exterior girders. Cross-frames were placed within the specimen portion of the bridge at 0.25$L$, 0.5$L$, 0.75$L$ (where $L$ is the span length of the bridge specimen) and at the ends for stability considerations. The cross-frames were constructed from $L76 \times 76 \times 9.5$ stock and welded in place in an 'X' configuration. Cold rolled bars, milled 6.4 mm off the top to ease in welding to the bottom side of the bottom flange, were connected to the girders to mimic a simply supported condition. The end supports, intended to idealize roller supports, were placed on stainless steel plates.

## 4. Joining technique for the hybrid deck system

Effective joining techniques represent one of the challenges facing the use of FRP decks. There is limited literature available that discusses connection techniques for many types of decks and the proposed deck is no exception. It is well recognized that component-to-component connection, panel-to-panel connection, and deck-to-support system connection represent some of the most outstanding obstacles that require careful investigation to improve the acceptance of FRP's in bridge construction. Zhou and Keller [29] documented the technical background, development and design guides of FRP bridge deck connections, and design principles concerning the joining of FRP decks. Joining techniques pertaining to panel-to-panel connections and deck-to-support connections for the proposed hybrid deck are discussed in the following subsections.

### 4.1. Panel-to-panel connections

Panel level connections are necessary to efficiently transfer bending moment and shear forces between jointed panels, provide resistance to dynamic loads, and ensure deformation compatibility. Panel-level connection techniques include adhesive bonding and mechanical fixing. Mechanical fixing includes shear keys, splicing tongue–groove connections, and clip-joints. Mechanical fixing has the advantage of easy assembly. However, load transfer and failure resistant capability of mechanical fixing is not as efficient as bonded joints [29]. Results from constructed projects with shear key connection show that cracks appeared after a period of exposure to highway vehicle loadings [25]. The cracking at the shear key connection region shows that mechanically fixed connections are not reliable to resist dynamic vehicle loadings. Zetterberg et al. [28] proposed two different joining techniques for pultruded composite profiles for bridge deck applications. They used both adhesively bonded and bolted joints for panel-to-panel connections. Their analytical results showed that the bonded joint is likely to always be easier to design and will be more amendable for realization.

In this study, adhesively bonded connections were used to maintain the integrity of the panel-to-panel connection. By using a detailed finite element model, as will be discussed later, it was found that the maximum transverse shear stress at the interface between adjacent panels of the proposed hybrid deck was 5.44 MPa under service loads (1× tandem load) that is smaller than the shear strength of commercially available resin, which ranges from 10.35 to 34.5 MPa [5]. However, the main disadvantage of bonded connections is the difficulty in applying and controlling the quality of the bond in the field.

### 4.2. Connection of hybrid deck on steel girders

For system-level connections, shear transfer and connection constructability are the major issues that we addressed in this research. One of the challenges with the proposed hybrid deck is the development of a reliable connection between the deck and the steel girders. So far, and to our knowledge, there is limited number of FRP bridges built world-wide constructed compositely with steel girders. Alternatively, considerable number of FRP decks constructed in the last decade were designed and constructed without accounting for any composite action with the supporting steel girders. The degree of composite action significantly affects the behavior of the composite section of the bridge. If there is no composite action and the section is subjected to some arbitrary vertical loading, the bottom surface of the deck is in tension whereas the top surface of the beam is in compression, which is inherently a slip that occurs between the two surfaces. If partial composite action exists, the slippage will be reduced. However, full composite action is often desired where slip is prevented.

Mechanical fixing techniques, adhesive bonding, and hybrid joints that combine both mechanical and adhesive bonding have been used to connect FRP decks to steel girders [29]. Mechanical fixings include stud-type connections, clamped connections and bolted connections. Depending on the requirements of a specific project, the deck-girder connection can be a permanent joint with composite action, or an easily constructed connection that provides no composite action between the deck and its supports such as clamped connection detail. In a case where composite action is required, the efficiency of shear transfer and constructability are major factors influencing the design of the connection.

Clamped connection is effective for preventing uplift of the panels. Meanwhile, clamped connection does not develop composite action between deck and the supporting girders. The clamp device is also fairly labor intensive, as the connection needs to be installed from underneath the bridge deck. Kansas Structural Composites, Inc., (KSCI) manufactures a sandwich FRP deck with a sinusoidal honeycomb type FRP core. They have adopted a clamped connection for these panels for bridge applications [20]. The connections are placed at panel-to-panel joints. Each joint contains an FRP tube through which holes are drilled and bolts installed to secure a clamping device.

Bolts have been used occasionally to provide a connection between FRP decks and girders [18], and are installed typically inside of steel sleeves through matched holes drilled through the entire depth of the deck and the top flange of the girder. Bolts are installed from beneath top flange of the girder. Park et al. [24] presented a new connection method for deck-to-girder connections of GFRP decks. They proposed a mechanical connection using bolts, and concluded that the anchor bolt diameter should be at least 20 mm and recommended an edge distance of between $1.4D$ and $2.0D$ times the bolt diameter. Kim et al. [16] proposed bolted connections for deck to concrete girder connection. The proposed deck-to-concrete girder connection by Kim et al. [16] is suitable for the deck renewal projects.

Adhesive bonding has the advantage of high strength and good corrosion resistance. When the deck supports are wide and flat, it is possible to use an all-adhesive connection. In this case, adhesive bonding is preferable to hybrid connecting mainly because fewer steps are involved in the bonding process and connector forces are evenly distributed along the joint. Keller and Gurtler [14] showed that adhesive bonding between FRP bridge deck and steel girders behaved well under quasi-static and fatigue loading. The connection did not fail and showed no damage after 10 million cycles of loading. Keller and Gurtler [14,15] tested two large scale hybrid girders consisting of FRP bridge decks adhesively connected to steel beams. Response of the two girders was studied at the service and failure state. Their experimental results showed that the adhesive connection between GFRP bridge decks and steel girders behaved well under creep loading.

Headed shear studs are routinely used to provide shear continuity across the steel- concrete interface of steel-concrete composite beams in buildings and bridges. Creative Pultrusions, Inc., Martin Marietta Composites (MMC), and hardcore composites (HC) are three manufacturers of FRP bridge decks that have used shear-stud type connections [18,19]. Moon et al. [23] investigated three different shear studs connections between steel girders and the MMC Gen4 FRP deck through static and fatigue testing. Static test results suggested that a larger volume of concrete surrounding the shear studs decreased the stress concentration directly behind the shear studs and alleviated local crushing. Moon et al. concluded that approximately 60–70% of the capacity of a longitudinal connection in a continuous concrete deck was developed with this connection. This decreased capacity was due to failure modes related to the discrete nature of FRP decks. Righman et al. [26] proposed a clamped shear stud connector for FRP decks to steel stringers. Their connection consisted of a threaded shear stud welded to the top flange of the supporting girder and housed inside steel sleeves that were installed within a hole drilled through the FRP deck. The performance of their connector was verified through experimental testing of a reduced scale bridge. Reising et al. [25] summarized installation issues for four FRP panel systems installed in a 207 m, five-span, and three-lane bridge. All panels were delivered to the site with pre-drilled stud at 1.2 m intervals; 18 cm studs were welded onto the girders through the stud holes. By monitoring the response of the bridge over a period of 2 years, they observed that the thermal characteristics of the FRP panels, which resulted in unexpected uplifts and significant thermal gradient, are mainly responsible of the vertical displacement of the panels related to the girders.

The proposed hybrid deck, which was investigated in this study, should serve as transverse load-carrying element as top chord in composite bridge. After studying the performance and installation issues for different connections, which were described earlier, it was decided that a welded shear stud connection is the most efficient for an enhanced system-level performance. Implementing familiar shear stud technology enables the design to be both easy to install and cost effective. Construction of this connection involved: welding the threaded studs to the girder in clusters to avoid excessive drilling in the deck. Then, a 0.05 m diameter holes were drilled at each cluster of studs through the top and inner flange of the hybrid specimen for concrete pouring. In addition, rectangular with semicircle holes were drilled through the bottom face of the specimen. The holes were then blocked off with foam inserts. Subsequently the hybrid deck was placed on the girders. Holes were then filled with non-shrink concrete and covered with the FRP cutouts by applying an adhesive resin to protect the cutout region.

AASHTO LRFD 1998 has design specification for shear studs for only concrete decks. FEA was used in this study to design the shear studs. The averaged horizontal shear force between the hybrid deck and the steel girders were obtained from the FEA results. Then, number of the required shear studs to resist that shear was calculated. Hence, eight (12.7 mm) diameter (101.6 mm) height stud connectors were used and distributed in certain locations along the entire span. Longitudinal shear studs spacing is specified in Fig. 2. The shear studs connectors, which were used in this study, intended to provide composite action between the hybrid deck and steel girders. Composite action of the hybrid deck offers two main advantages: (1) the overall stiffness and load resistance capability of the hybrid deck system can be significantly higher when compared to its individual girders; (2) the overall bridge system

can have ductile characteristics since the girder is made from ductile material (steel) and by the utility of efficient load transfer between the brittle hybrid deck and its ductile girders, and thus renders the system the desired ductility.

## 5. Effective flange width

Under positive bending moment, part of the hybrid deck will act as the compression flange of the steel girder. When the spacing between the girders becomes large, beam theory does not apply because the longitudinal compressive stress in the flange will vary with the distance from the girder web [4,9]. Due to the action of in-plane shear strain in the flange of the composite girder under flexure, the longitudinal displacements in the parts of the flanges remote from the webs lag behind those near the webs and this phenomenon is called ''shear lag''. Shear Lag can lead to inaccurate estimation of the deflections and stresses in the flange, based on the simple beam theory as stated by Moffatt and Dowling [22]. For the shear-lag phenomenon in slab-on-girder structures, the concept of an effective flange width was introduced many years ago, for conventional reinforced concrete, to provide a simple procedure to indirectly address shear lag in T-shaped beams. Four factors influence the effective width of concrete flanges for composite beams: (1) span; (2) beam spacing; (3) degree of interaction between slab and beam; (4) pattern of loading [11]. Codes implement different approaches for specifying effective flange width. There is no guidance as for the effective width for composite FRP-steel girders at this time.

Keelor et al. [13] conducted a field study of a FRP deck-steel girder composite bridge in Pennsylvania. The bridge employed a cellular FRP deck system that was attached to the steel girders by headed shear studs and grouted in place within the FRP cells using a non-shrink grout. The bridge was instrumented and was subjected to a series of service loads. The data were collected and used with standard transformed section calculations to identify appropriate effective widths. Keelor et al. observed that FRP decks and floors acting compositely with underlying steel girders exhibited an effective width, at the service condition, of approximately 75% of the girder spacing for interior girders and 90% of the total distance, made up of the girder spacing added to the deck overhang, for the case of exterior girders.

Guidelines for hybrid FRP effective widths are useful in the design of fully composite hybrid deck-steel girder installations. In our investigation of the composite action, we only considered the service load condition. The service load level is important for the case of hybrid deck-steel girder composite construction since the ultimate strength performance of such systems is currently not known and hence frequently not considered in design. However, the service load composite response of these systems is frequently assumed to hold and hence the composite cross-section is considered when computing live load deflections. However, the ultimate behavior of the system presented herein will be tested in the near future. To support the notion of effective flange width design approach, we examined the bridge system analytically and experimentally to derive appropriate values. The data were collected from experimental results (to be discussed later), and then used with standard transformed section calculations to identify appropriate effective flange widths. Effective width ratio can be defined as the ratio between the effective flange width to the girder spacing for interior girder installations, and to the total distance, made up of half of the girder spacing added to the deck overhang, for the case of exterior girders.

### 5.1. Transformed section calculations

Based on the upward shift in the measured steel girder neutral axis location, it is possible to compute the level of composite action that the hybrid deck provided in resisting the internal moments needed to equilibrate the tandem loadings. The strain gages data of the steel girders obtained from test results under service loads were used to determine the neutral axis location for the steel girders. Using this approach, it is then possible to back-calculate the hybrid deck effective compression flange width using standard transformed section properties related to the modular ratio of steel to both FRP and concrete.

Fig. 3 depicts the idealized cross-section that was used for calculating effective width for service loading computations. It was assumed that only a portion of the hybrid deck cross-section is effective in resisting the compressive stress that develops during the formation of the internal equilibrating moment of the composite cross section. The hybrid deck considered in this study was made of hollow trapezoidal tubes bonded together and oriented such that the tubes are perpendicular to the steel girders longitudinal axis. Because of this we assumed that, due to voids inside the tubes, only the top, inner flange, and bottom FRP face

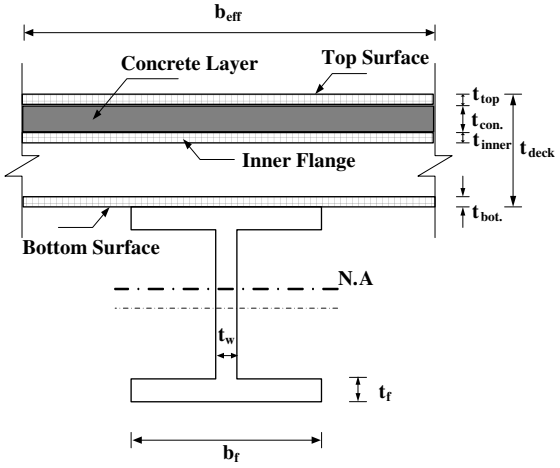


Fig. 3. Idealized cross-section of the transformed section of the bridge.

sheets along with the concrete layer that are in continuous contact across tube interfaces, and thus represent the only contiguous elements within the hybrid deck. A detailed discussion of the transformed section calculations and the validation of this assumption via the experimental results are documented in [2].

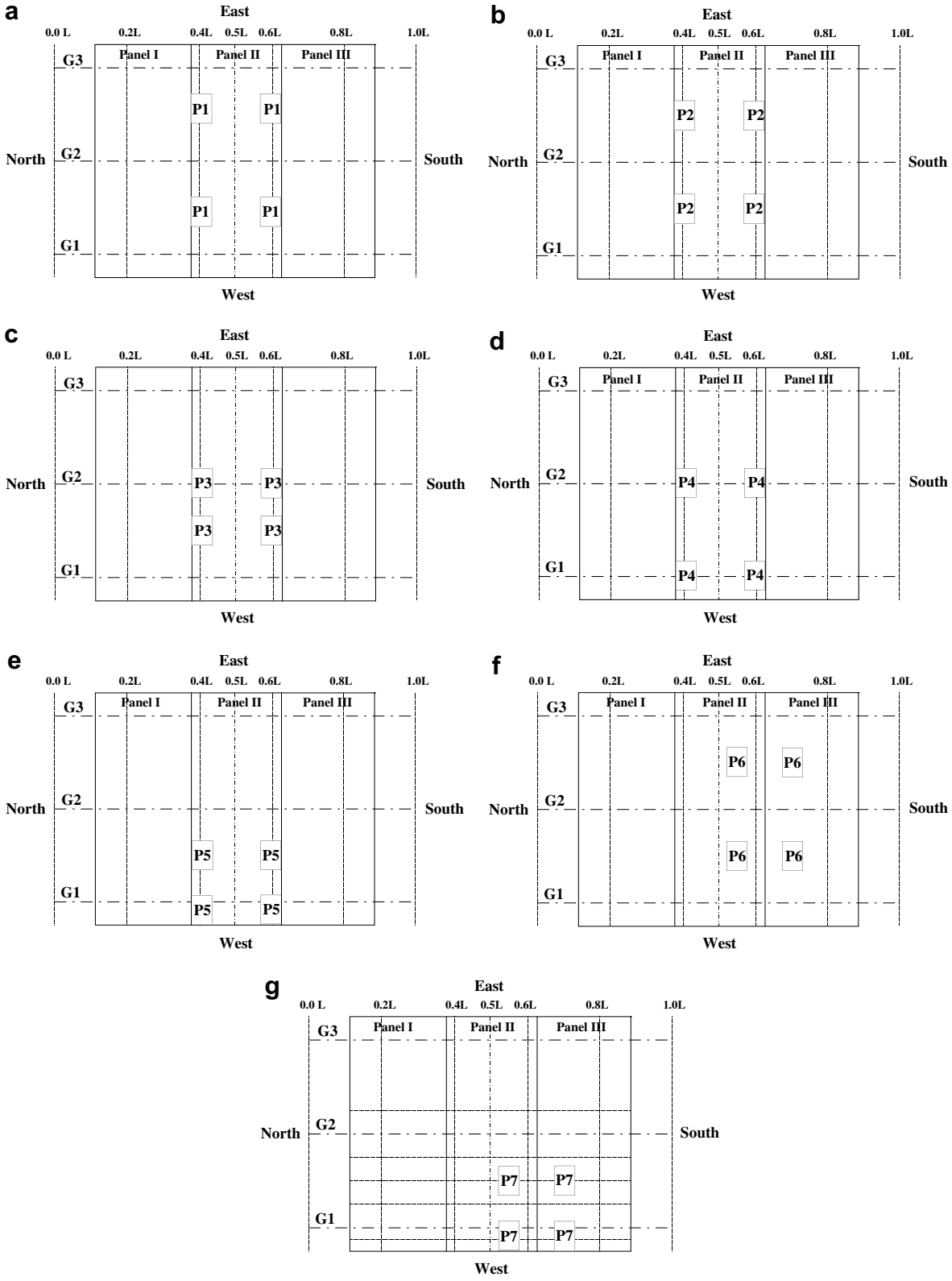


Fig. 4. Seven service load cases (a) case 1, (b) case 2, (c) case 3, (d) case 4, (e) case 5, (f) case 6 and (g) case 7.

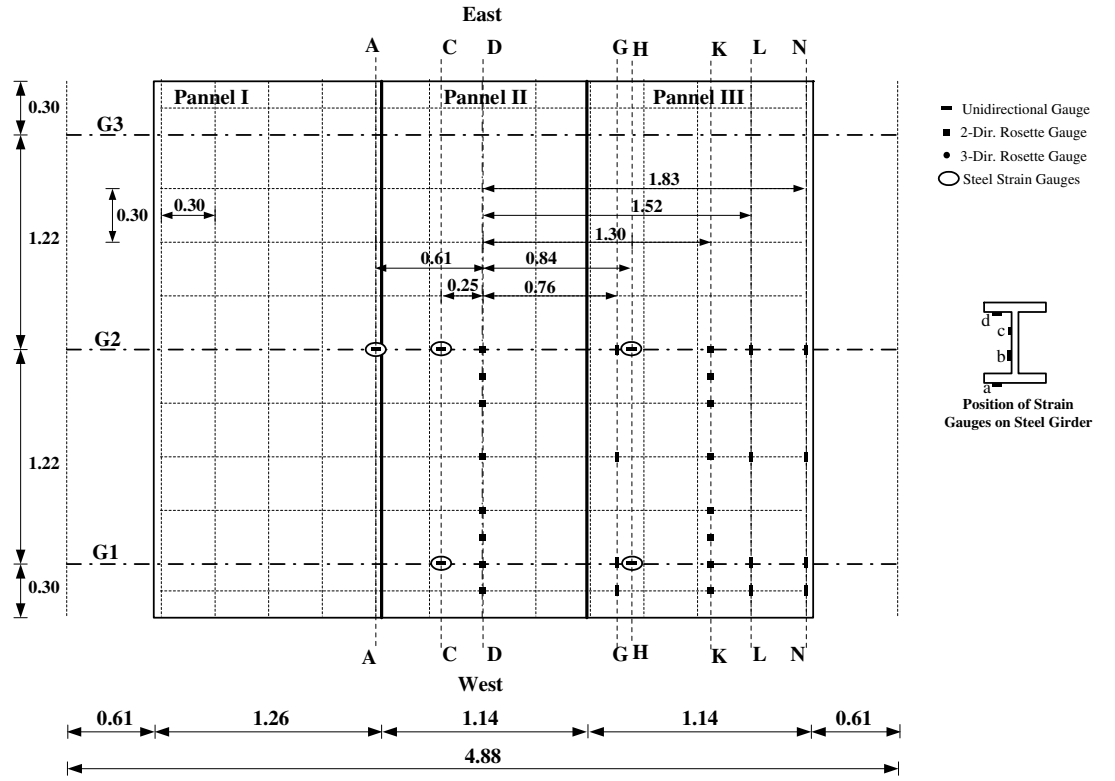


Fig. 5. Strain gages locations for deck top surface and steel girders (dimensions in metres).

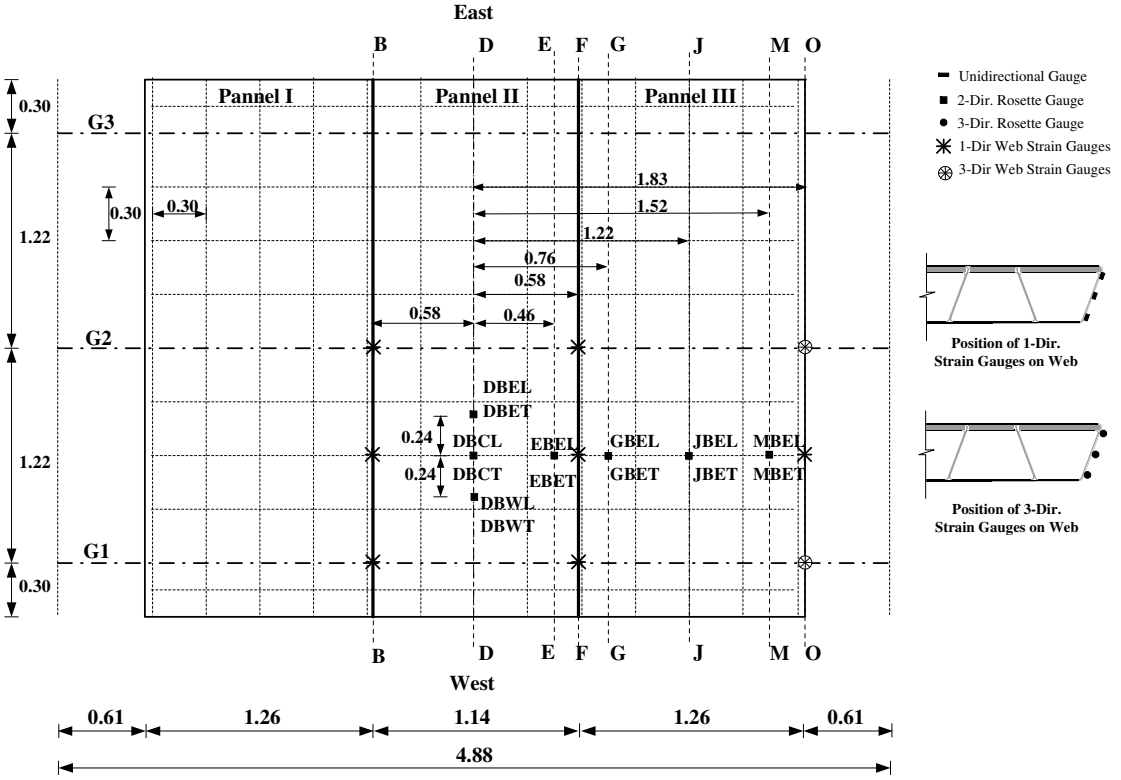


Fig. 6. Strain gages locations for bottom surface and webs of the hybrid deck (dimensions in metres).

## 6. Experimental program

The objectives of the experimental investigation are three-fold: (i) capturing the global response of the specimen subjected to a series of service flexural loading conditions, (ii) investigating the shear connections, and (iii) providing guidelines for computations of effective flange widths to be employed in the design of this particular FRP-concrete deck system. The maximum load applied to the specimen was 123.75 kN, which represented (1× tandem load).

Fig. 4 shows the service loading cases. The locations at which the load was applied for each case are identified by the four boxes in the figures. Case 1 was designed to simulate the tandem load specified in the 1998 AASHTO LRFD Bridge Design Specifications. Cases 2 and 3 were designed to determine the governing case for the interior girder. Case 4 was intended to maximize the shear lag over the girders. Case 5 is sought to identify the governing case for an exterior girder. Cases 6 and 7 are identical to cases 2 and 5 with the design tandem shifted to $0.62L$ to examine the behavior and structural integrity of panel-to-panel joints. The maximum load for each case was repeated three times to verify the consistency if the test results.

### 6.1. Experimental set-up

Fig. 7 shows service load test fixture and the three simply supported steel girders (W $760 \times 284$). Loads were applied to the top surface of the test specimen by the compression stack beam connected to a pair of actuators attached, which were anchored to the strong floor. In the transverse direction, the actuators were stabilized by a steel box. The test configuration simulates the tandem load specified in the 1998 AASHTO LRFD Bridge Design Specifications. The design tandem load is defined as a live load that has two axles of 110 kN. One axle is 1.2 m away from the

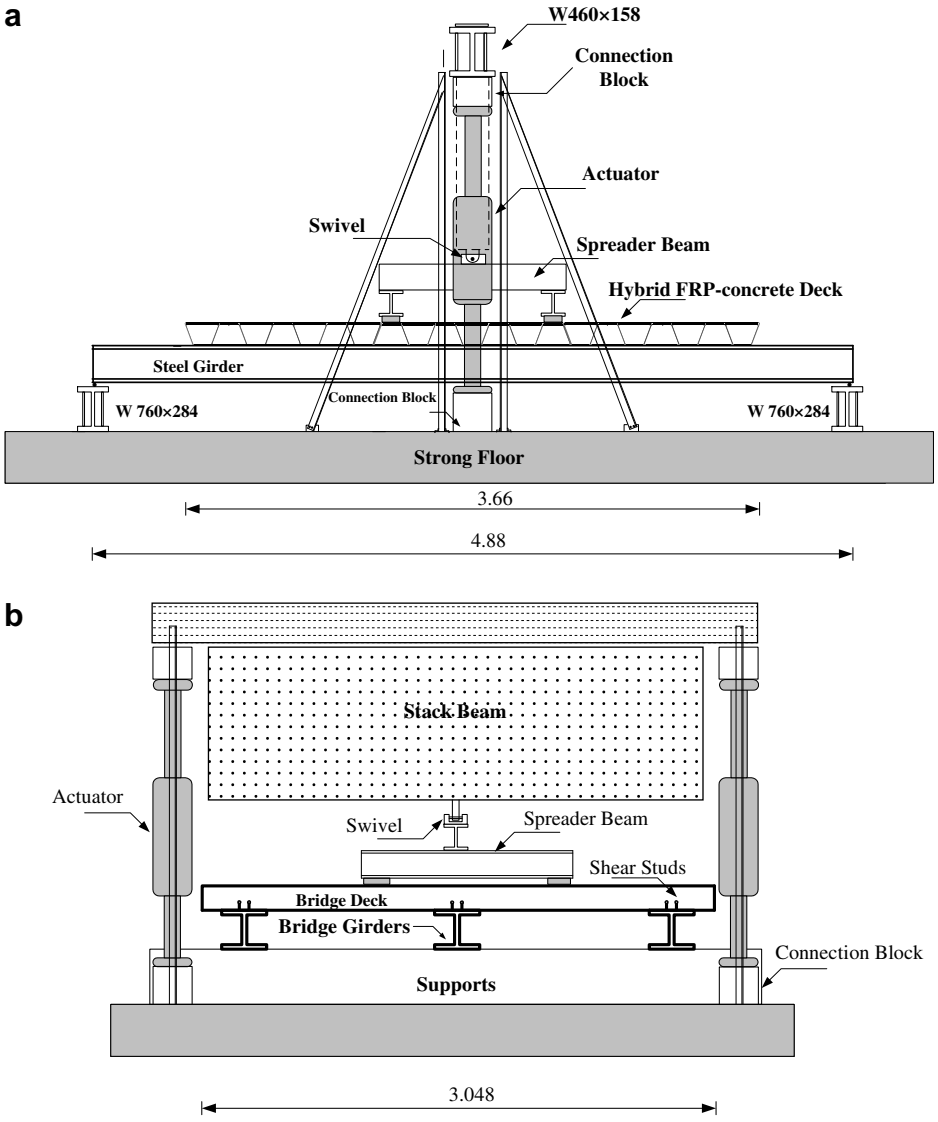


Fig. 7. Test configuration for service test (dimensions in metres) (a) longitudinal elevation and (b) transverse elevation.

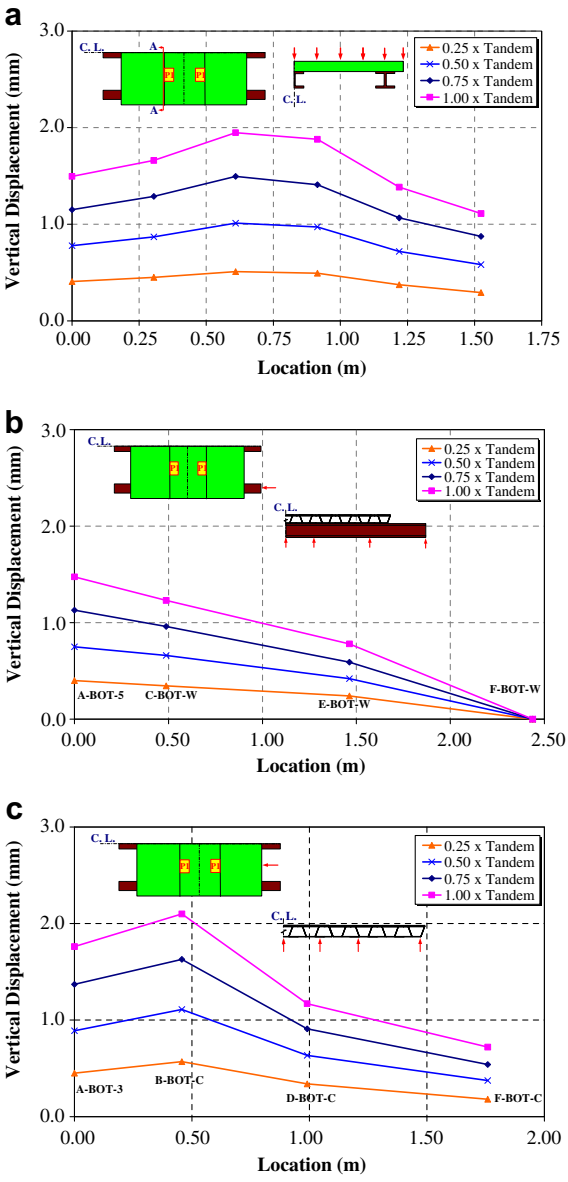


Fig. 8. Deformed shapes at different load levels under load case no.1 (a) section A, top surface, (b) exterior girder-bottom surface, and (c) bottom surface-longitudinal direction.

other. Each axle has two tires that are 1.8 m center-to center. Each tire area is 0.510 m wide and 0.385 m long. For the 3/4 scale model, this design tandem load becomes two axles of 61.875 kN 1.35 m apart. The two tires of each axle are 0.9 m apart and each tire area is 0.383 m wide and 0.289 m long. To simulate the tire areas, four steel plates covered by rubber with the same area as the scaled tire area, were attached to the bottom face of the spreader beams.

### 6.2. Instrumentation

Various instruments (strain gages, potentiometers, etc.) were used to capture the specimen behavior during testing. Only a quarter of the test specimen was instrumented due to symmetry. To acquire a good resolution of the deck shear lag in the positive moment regions for service loading, strain gages were located at several cross-sections along the span of the specimen. The layout of the strain gages on the top surface of the hybrid deck is shown in Fig. 5. A significant number of gages were placed at the midspan of the specimen since one objective of this experiment was to investigate the behavior of cross-sections that would achieve maximum strain during loading. A significant number of gages were placed along girder 1 and 2 to provide information on composite action. Another transverse line of strain gages was placed at $0.77L$ from bridge support to provide data at locations away from the point loads (i.e. way from local effects). Other gages were placed to provide data to plot the strain profile through the thickness of the deck.

Few gages were placed on the bottom surface of the hybrid deck to provide information on the strain variation in plan and across the width of the deck. The layout of strain gages on the bottom surface of the hybrid deck is shown in Fig. 6.

To measure the slip between the hybrid deck and girder, and between the concrete box holding the shear studs and the deck, during the service tests, slip gages were installed along the central girder and one of the two edge girders at midspan. The readings from these gages represent the relative displacement between the deck and the girder. This study did not focus on distribution of load to girders; therefore, load cells were installed above the spread beam to capture the force being applied to the specimen.

### 6.3. Test results and discussion

Selected results for all seven different service loading cases are presented in this section. Visual inspection after each loading case revealed no cracking or delamination in the exterior GFRP laminates. Moreover, there was no trace of damage in the shear connectors as evident by the fact that there was no slip between either the hybrid deck and the girders, or the concrete box (holding the shear studs) and the deck during the service load evaluation.

#### 6.3.1. Stiffness and strength behavior

From the series of service tests, the maximum displacements and strains at different location of the specimen were extracted from test data. The deformed shapes of the top surface of the specimen under service load case 1 are shown in Fig. 8. The displacement was greatest at the point closest to the loading point, which is clearly depicted in Fig. 8a. All three panels show near linear relationships between force and displacement, which indicates that the hybrid deck can be modeled with a linear material behavior for service loads. According to AASHTO [1], the maximum deflection under (1+IM) × truck load should not exceed $L/800 = 6.10$ mm, where $L$ is the span length. However, the (1+IM) × tandem load was used here for comparison

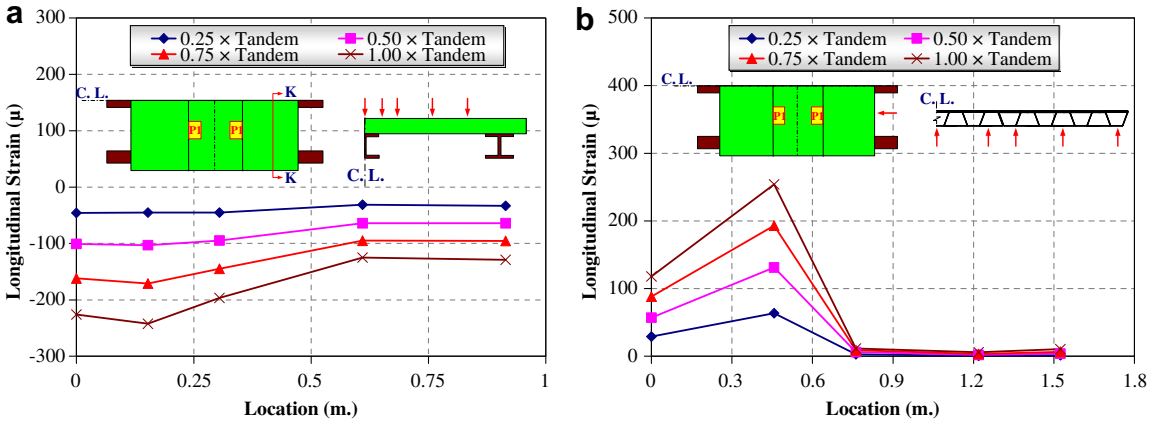


Fig. 9. Strain profile at different sections of the deck under load case no. 1 (a) section K, longitudinal and (b) longitudinal strain.

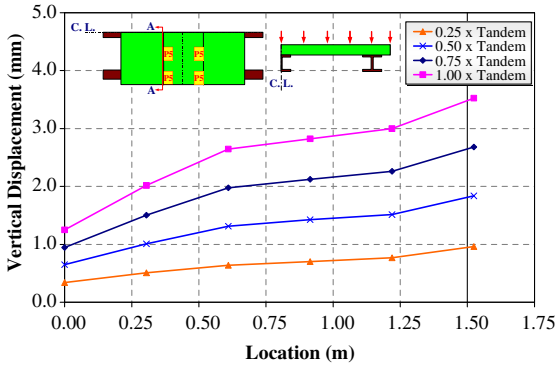


Fig. 10. Deformed shape of the deck at different load levels under load case no. 5.

since the loading configuration in the test simulates the tandem load. One can see from Fig. 8c that the deformation in the hybrid deck measured at B-BOT-C due to (1+IM) × tandem load was 2.79 mm (0.46*L*/800). This hybrid deck easily satisfied the AASHTO live load deflection limit. Displacements of the exterior steel girder are shown in Fig. 8b. The maximum deformation at the midspan of the exterior steel girders measured at A-BOT-5 due to (1+IM) × tandem load was 1.96 mm (0.32*L*/800).

Fig. 9 shows the measured longitudinal and transverse strains at different cross-sections of the specimen under service load case 1. The longitudinal strain along section K is not uniform because of the shear lag and is clearly shown in Fig. 9a. Fig. 9b shows the longitudinal strains measured along the centerline of bottom surface. At the load level of 1× tandem load, the strain measured at location DBCL was 254 μ, which is very small when compared to the averaged ultimate strain of FRP composites considered in this study (i.e. 25,000 μ). By examining the behavior of the specimen under service load case 5 shown in Fig. 10, the deformation in the overhang of the hybrid deck due to (1+IM) × tandem load was 4.66 mm (0.76*L*/800). The overhang of the hybrid deck also satisfied the AASHTO live load limit.

Overall, the test specimen satisfied both the stiffness and strength limits. Furthermore, test results showed that the design of the proposed hybrid bridge deck is still stiffness-driven.

### 6.3.2. Composite action behavior

The specimen was instrumented to capture the composite action taking place between the hybrid deck and steel girders. Fig. 11 presents the strain variation along the interior and exterior steel girders at sections C and H under service load case 5. The location of the neutral axis obtained from the test clearly shows a shift upward due to the composite bending action between the hybrid deck and the underlying steel girder, but did not move as the load was increased from 0.25× tandem to 1.00× tandem. The strain variation through the steel girders was used to calculate the location of the neutral axis for each of the two instrumented cross-sections in the interior and exterior girders. Based on the upward shift in the neutral axis location from the centroid of the steel girder alone, it is a simple exercise to compute the contribution of the hybrid deck to the internal moment and the effective compression flange width. The results summarizing the composite action are given in Table 4 for both interior and exterior girders. Based on these results, it was observed that the hybrid deck, exhibits partial composite action with the steel girders. This partial composite action translates into an effective width, at service condition, of approximately 46% of the girder spacing for the interior girder installations, and 50% of the half of the girder spacing and the deck overhang for the exterior girders.

Fig. 12 shows the measured longitudinal and transverse strains along different cross-sections of the specimen under load case 2. Again, the longitudinal strain along section K of the deck is not uniform as a result of shear lag. The measured strains correlate well with those of service load case 1. This confirms that the measurements were consistent. The measured strains on the interior web at sections F-East (refer to Fig. 6 for location) is clearly shown in Fig. 12b. This figure confirms that the plane section before deformation remains plane and normal to mid-plane after deformation, which validates the assumptions we used to calculate

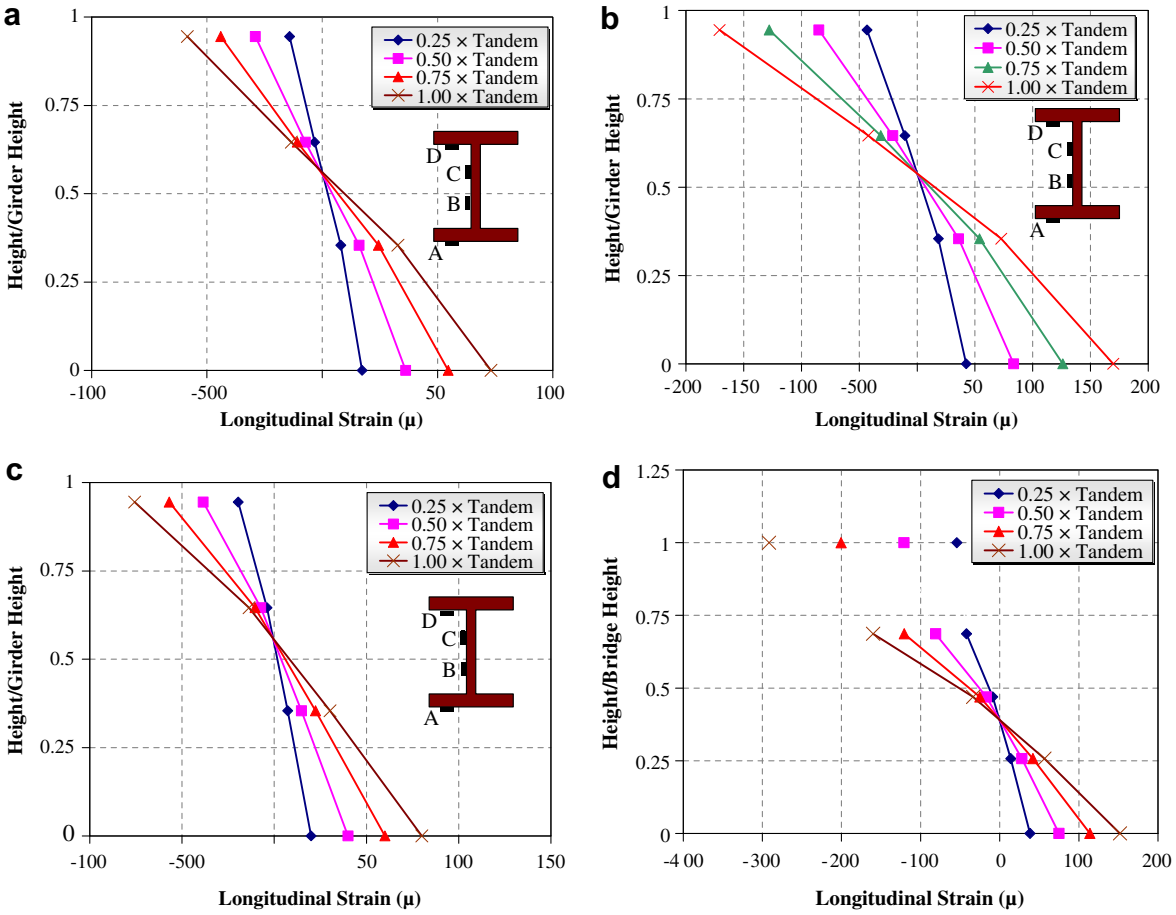


Fig. 11. Strain profile through different sections under load case no. 5 (a) section C, interior, (b) section C, exterior, (c) section H, interior and (d) section H, exterior.

the effective flange width of the hybrid deck by using Euler–Bernoulli beam theory. The location of the neutral axis of the hybrid deck obtained from the test again for this case shows a shift upward due to the presence of the concrete layer in the compression zone and the partial composite action.

Service load case 6 is identical to service load case 2 with the exception that the load was applied at $0.62L$ (where $L$ is the bridge span length). The measured longitudinal and transverse strains along different cross-sections of the specimen under service load case 6 are clearly shown in Fig. 13. Fig. 13a presents the transverse strains measured along section G. The longitudinal strains measured along the centerline of the hybrid deck are unbroken, indicating that adjacent deck panels were acting together rather than as separate pieces. This suggests that the adhesive connection between panels is providing adequate transfer of load between the adjacent panels.

## 7. Finite element analysis

An analytical study of the scale-model bridge was performed. The objective of the analytical study was to develop finite element models of the bridge that accurately predict structural parameters such as deflections and strains, and to be compared with the experimental results. The modeling techniques, if validated, could be used to design hybrid bridges and further investigate the response beyond the service loading condition. The general purpose finite element analysis software, ABAQUS [12], was used in the finite element analysis.

Table 4
Effective flange width ($b_{eff}$), and effective flange width ratio ($b_{eff}/b$) for interior and exterior girders

| Service load case | Interior girder, $b_{eff}$ (m) | Interior girder, $b_{eff}/b$ | Exterior girder, $b_{eff}$ (m) | Exterior girder, $b_{eff}/b$ |
|---|---|---|---|---|
| Case 1 | 0.558 | 0.46 | 0.559 | 0.61 |
| Case 2 | 0.532 | 0.44 | 0.53 | 0.58 |
| Case 3 | 0.637 | 0.52 | 0.53 | 0.58 |
| Case 4 | 0.595 | 0.49 | 0.43 | 0.48 |
| Case 5 | 0.584 | 0.48 | 0.37 | 0.4 |
| Case 6 | 0.506 | 0.42 | 0.45 | 0.49 |
| Case 7 | 0.506 | 0.42 | 0.34 | 0.37 |
| Average | 0.559 | 0.46 | 0.46 | 0.50 |

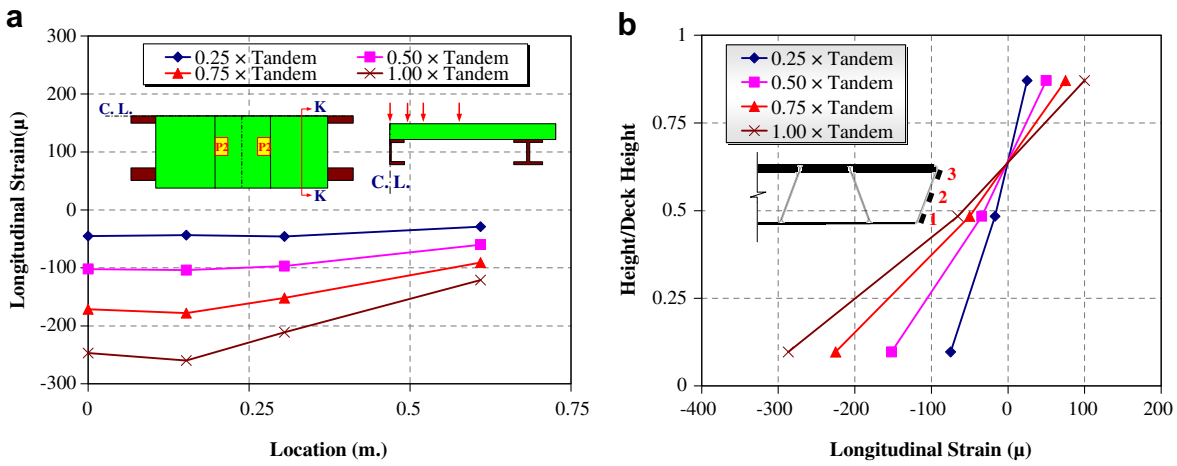


Fig. 12. Strain profile through different sections of the deck under load case no. 2 (a) section K, longitudinal and (b) section F, East.

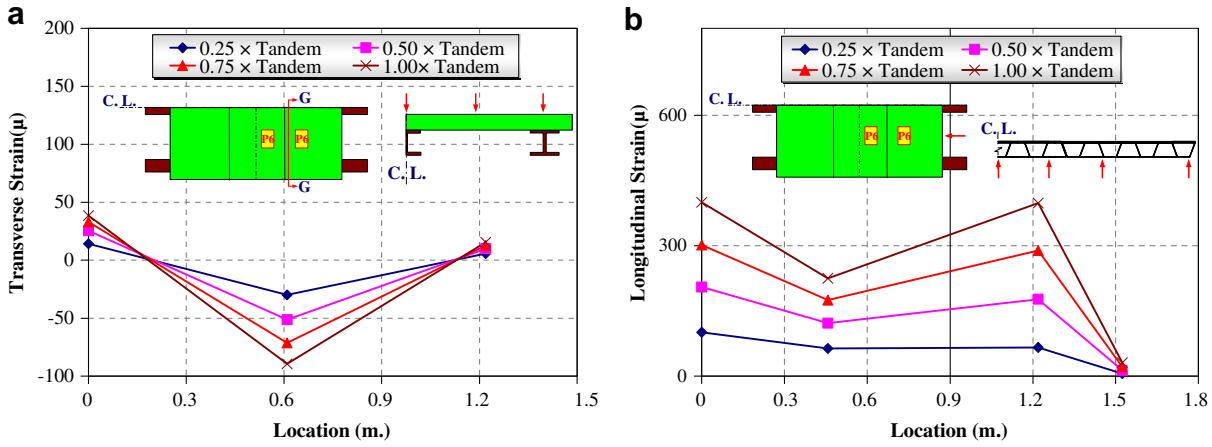


Fig. 13. Strain profile through different sections of the deck under load case no. 6 (a) section G, transverse and (b) longitudinal strain.

### 7.1. Geometric, boundary condition, and material modeling

Shell elements were the principal element type used since the bridge deck was made of thin GFRP laminates. The reduced integration S4R5 element (4-node doubly curved thin shell element; each node with five degree of freedom) was used to model the thin GFRP laminate. The continuum or solid element C3D8R (8-node linear brick with reduced integration) was used to model the concrete. Steel girders were modeled in a similar manner as the concrete layer, using a continuum element with reduced-integration formulation.

The area between the girders and deck was modeled using contact elements. The girder top surface was assumed to be the master surface, while the deck bottom surface was assumed as the slave. The connection between the girders and deck was assumed as fully composite at the locations where these connections existed in the physical model. By using a composite bond in the connection modeling, bond-slip effects cannot be detected. However, only a static monotonic loading was considered in the analysis, and overall global behavior is considered more significant than local effects such as bond-slip in this investigation. Perfect bond between the deck panels was assumed in all analyses carried out in this study. The finite element model of the prototype hybrid FRP-concrete bridge deck model is shown in Fig. 14.

A linear finite element model can predict the behavior of a hybrid bridge with sufficient accuracy if the strain induced in the materials is within the strain ranges where the elastic moduli of the materials were obtained. The concrete, steel, and GFRP were shown to behave nonlinearly in the higher strain ranges. However, material nonlinearity was not considered in this study because for this stage of the experimental investigation because strains in the material remained in the linear elastic range. The prediction of failure and response at ultimate state is to appear in a subsequent paper.

### 7.2. Validation of FE analysis with experimental results

Fig. 15 shows the deformed shapes of the top surface obtained from the experiments and the linear FE analysis

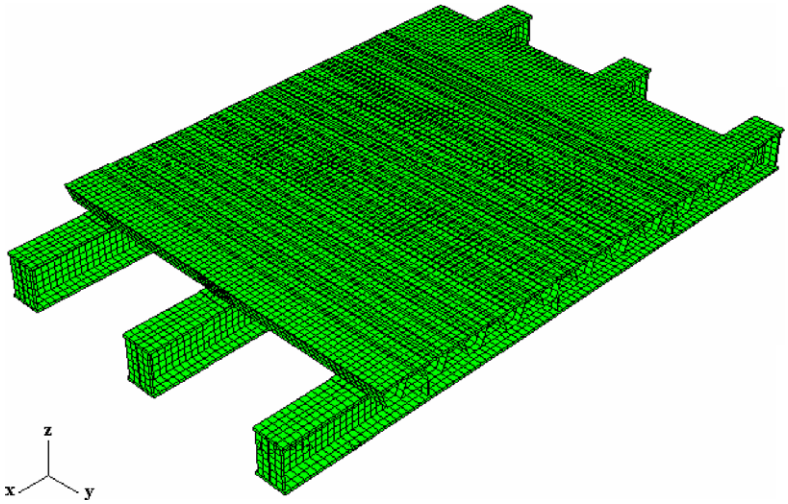


Fig. 14. Finite element model of the prototype bridge deck.

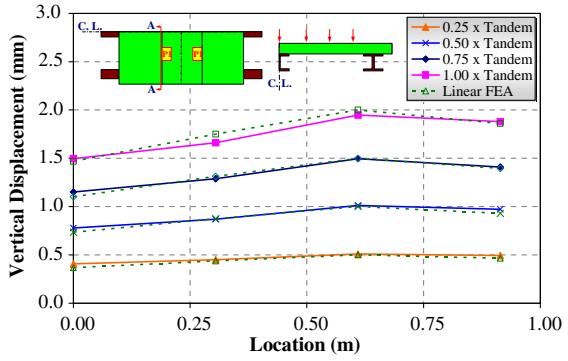


Fig. 15. Deformed shapes at section A under load case no. 1.

under load case no. 1. The FEA predicted the deformed shape in the test specimen relatively well, although there are small discrepancies at locations close to the loading points because of local deformations and the material models used for this stage of the analysis. Fig. 16 depicts the deformed shapes of the bottom surface of the inner girder under load case no. 3. Finite element analysis results exhibit a larger global flexibility when compared with the

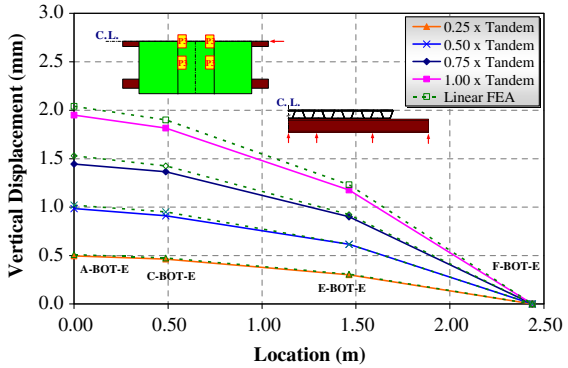


Fig. 16. Deformed shapes under load case no. 3.

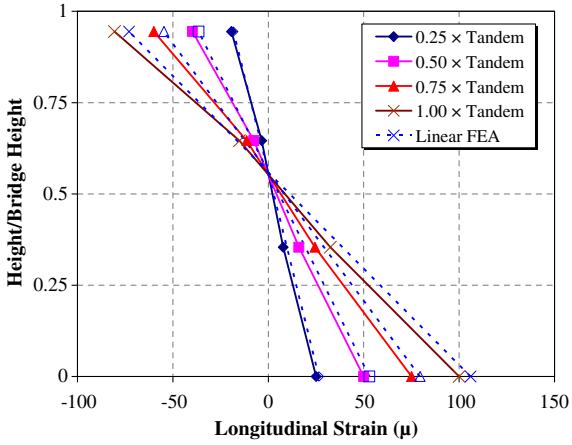


Fig. 17. Strain profiles through the interior steel girder at section H under load case no. 2.

experimental results. However, the difference between the two results is not significant. Overall, the finite element response correlates well with the test results.

Fig. 17 presents strain profile through steel girder under load case no. 2 at section H. A negative value indicates compressive strain, while a positive value indicates tensile strain. The correlation between the FEA results and experimentation are very good, especially at the bottom flange of the girder.

## 8. Conclusions and recommendations

A hybrid FRP-concrete deck on steel girders specimen was subjected to a series of service flexural loading tests. Seven different loading conditions were considered to capture the global response of the specimen, and to investigate the composite action of the bridge. The experimental results demonstrated the excellent performance of the hybrid FRP-concrete bridge deck under service loads.

This hybrid deck specimen satisfied the AASHTO live load deflection limits. Linear FEA was found to predict accurately the flexural behavior of hybrid bridge systems in the elastic range. Therefore, linear FEA is a good tool in the design stage of the hybrid bridge systems.

The proposed hybrid deck acting compositely with steel girders exhibited an effective width, at service condition, of approximately 46% of the girder spacing for the interior girder installations, and 50% of the half of the girder spacing and the deck overhang for the exterior girders. Effective width calculations of the hybrid deck showed that the effective flange width for hybrid decks are less than AASHTO prescribed effective width for concrete decks. However, this result is only applicable to the hybrid bridge studied herein. A parametric study should be conducted with different span lengths, different cross sectional heights, girder spacing, and skew angle, to generalize the results obtained herein.

## Acknowledgements

The work in this paper was conducted in collaboration with New York State Department of Transportation (NYSDOT). The views presented in this document represent those of the authors and not the NYSDOT.

## References

[1] American Association of State Highway and Transportation Officials. AASHTO LRFD bridge design specifications. 2nd ed. Washington (DC): AASHTO; 1998.
[2] Alnahhal WI. Structural characteristics and failure prediction of hybrid FRP-concrete bridge superstructure and deck systems. Ph.D. Dissertation, The State University of New York, University at Buffalo; 2007.
[3] Alnahhal W, Chiewanichakorn M, Aref A, Alampalli S. Temporal thermal behavior and damage simulations of FRP deck. J Bridge Eng, ASCE 2006;11(4):452–65.
[4] Aref AJ, Chiewanichakorn M, Chen SS, Ahn I-S. Effective width definitions for negative moment regions of composite bridges. J Bridge Eng, ASCE 2007;12(3):339–49.
[5] Aref AJ. A novel fiber reinforced composite bridge structural system. Ph.D. Dissertation, The University of Illinois at Urbana, Champaign; 1997.
[6] Ashby MF. Overview no. 92—materials and shape. Acta Metallur Mater 1991;39(6):1025–39.
[7] Bakeri PA, Sunder SS. Concepts for hybrid FRP bridge deck systems, serviceability and durability of construction materials. In: Proceedings of the first materials engineering congress, vol. 2. Denver, Colorado: ASCE; August 13–15, 1990. p. 1006–15.
[8] Busel JP, editorProduct selection guide: FRP composite products for bridge applications. 1st ed. Harrison (NY): The Market Development Alliance of the FRP Composites Industry; 2000.
[9] Chen SS, Aref AJ, Chiewanichakorn M, Ahn I-S. Development of effective flange width design criteria. J Bridge Eng, ASCE 2007;12(3):325–38.
[10] Federal Highway Administration and Federal Transit Administration. Status of the nation's highways, bridges and transit: conditions and performance-report to congress, 2003. <http://www.fhwa.dot.gov/policy/2002cpr/report.htm> [October 03. 03].
[11] Elkelish S, Robinson H. Effective widths of composite beams with ribbed metal deck. Can J Civil Eng 1986;13(5):575–82.
[12] Hibbit, Karlsson & Sorensen, Inc. ABAQUS/standard user's manual, version 6.3. Hibbit, Karlsson & Sorensen, Inc.; 2002.
[13] Keelor DC, Luo V, Earls CJ, Yulismana W. Service load effective compression flange width in FRP deck systems acting compositely with steel stringers. J Compos Construct, Am Soc Civil Eng 2004;8(4):289–97.
[14] Keller T, Gurtler H. Quasi-static and fatigue performance of a cellular FRP bridge deck adhesively bonded to steel girders. Compos Struct 2005;70(4):484–96.
[15] Keller T, Gurtler H. Composite action and adhesive bond between fiber-reinforced polymer bridge decks and main girders. J Compos Construct 2005;9(4):360–8.
[16] Kim H, Hwang Y, Park K, Lee Y, Kim S. Fiber reinforced plastic deck profile for I-girder bridges. Compos Struct 2005;67(4):411–6.
[17] Kitane Y, Aref A. Static and fatigue testing of hybrid fiber-reinforced polymer-concrete bridge superstructure. J Compos Construct 2004;8(2):182–90.
[18] Lesko JJ, Hayes MD, Schniepp TJ, Case SW. Characterization and durability of FRP structural shapes and materials. Compos Construct: A Real 2001:110–20.
[19] Market Development Alliance of the FRP Composites Industry. Industry overview: overview of the FRP composites industry—a historical perspective. Market Development Alliance of the FRP Composites Industry, 2002. <http://www.madacomposites.org/Industry_Overview.htm> [Dec.03.02].
[20] Meggers D. Fiber reinforced polymer bridge decks—The Kansas experience. Rep. Prepared for the Kansas Department of Transportation (CD-ROM), Topeka, Kan, 2000.
[21] Mirmiran A, Shahawy M, Beitleman T. Slenderness limit for hybrid FRP-concrete columns. J Compos Construct 2001;5(1):26–34.
[22] Moffatt KR, Dowling PJ. British shear lag rules for composite girders. J Struct Eng 1978;104(7):1123–30.
[23] Moon FL, Eckel DA, Gillespie JW. Shear stud connection for the development of composite action between steel girders and fiber reinforced polymer bridge decks. J Struct Eng 2002;128(6):762–70.
[24] Park KT, Hwang HY, Kim HY, Lee YH, Kim SM. Deck-to-Girder Connections for GFRP Bridge Decks. In: Proceedings of the fourth international conference on the advanced composite materials in bridges and structures. Calgary, Alberta; July 20–23, 2004. Montreal: Canadian Society for Civil Engineering. p. 9.
[25] Reising R, Shahrooz B, Hunt V, Neumann A, Helmicki A, Hastak M. Close look at construction issues and performance of four fiber-reinforced polymer composite bridge decks. J Compos Construct 2004;8(1):33–42.
[26] Righman J, Barth K, Davalos J. Development of an efficient connector system for fiber reinforced polymer bridge decks to steel girders. J Compos Construct 2004;8(4):279–88.
[27] Seible F, Karbhari VM, Burgueño R, Seaberg E. Modular advanced composite bridge systems for short and medium span bridges. Developments in short and medium span bridge engineering '98. In: Proceedings of the fifth international conference on short and medium span bridges. Canadian Society of Civil Engineers: Calgary (Canada), CD-ROM; 1998. p. 431–41.
[28] Zetterberg T, Astrom BT, Backund J, Burman M. On design of joints between composite profiles for bridge deck applications. Compos Struct 2001;51:83–91.
[29] Zhou A, Keller T. Joining techniques for fiber reinforced polymer composite bridge deck systems. Compos Struct 2005;69(3):336–45.